Development of superabsorbent soy protein-based bioplastic matrices with incorporated zinc for horticulture

M. Jiménez-Rosado[1]*, V. Perez-Puyana[2], F. Cordobés[1], A. Romero[2], A. Guerrero[1]

[1]*Departamento de Ingeniería Química, Escuela Politécnica Superior, Universidad de Sevilla, 41011, Sevilla, Spain*

[2]*Departamento de Ingeniería Química, Facultad de Química, Universidad de Sevilla, 41012, Sevilla, Spain.*

*MERCEDES JIMÉNEZ-ROSADO

Departamento de Ingeniería Química

Escuela Politécnica Superior, Universidad de Sevilla,

41011, Sevilla (Spain)

E-mail: mjimenez42@us.es

Phone: +34 954557179 Fax: +34 954556441

This article has been accepted for publication and undergone full peer review but has not been through the copyediting, typesetting, pagination and proofreading process which may lead to differences between this version and the Version of Record. Please cite this article as doi: 10.1002/jsfa.9738

ABSTRACT

Background

The use of superabsorbent materials in horticulture has spread recently. These materials, which can retain water and release it as crops need it, have great advantages such as the efficient use of water in periods of drought. However, these superabsorbent materials are made of synthetic polymers, which present problems of degradability and, sometimes, also toxicity. For this reason, the main objective of this work is the development of biodegradable superabsorbent bioplastic (SAB) matrices using as raw material a soy protein isolate (SPI). In addition, zinc is incorporated into these bioplastic matrices as an essential micronutrient for plants, to increase their added value.

Results

The incorporation of zinc chelated with 2,2',2'',2'''-(Ethene-1,2-diyldinitrilo)tetraacetic acid (Zn EDTA) (a salt with which the micronutrient is incorporated) into soy protein-based bioplastic matrices improve their superabsorbent capacity and provided a controlled release of water and nutrients to the crops.

Conclusions

The results show the high potential of these bioplastic matrices for their use in horticulture as superabsorbent materials that can release nutrients in a controlled manner.

Keywords: bioplastic matrices, superabsorbent, soy, zinc, controlled-released, horticulture

1. Introduction

In recent years, the effects of global warming have increased considerably due to human activity, mainly due to the increase in carbon dioxide emissions, which have boosted the greenhouse effect[1]. One of the main impacts of this warming is the change in the periods of rainfall. In this sense, periods of drought become more noticeable and extensive, whereas the periods of rainfall, although scarce, record a large amount of precipitated water, which produces floods and destruction[2]. These changes are notoriously detrimental to horticulture, since crops need a regular supply of water, increasing the use of irrigation in these crops, which makes them more expensive[3].

One of the solutions to this problem is the use of superabsorbent polymeric (SAP) matrices, which are buried into farmland[4]. These materials are capable of absorbing and retaining large amounts of water without disintegrating (from 10 to 1000 times their weight)[5], thus being able to retain rainwater and supplying it to plants, directly in the roots, during periods of drought, that is, optimizing the water cycle[6].

Nowadays, commercial SAP matrices already exist, which are added to the land in order to retain water and release it in a controlled way according to the needs of the crops (Creasorb from Evonik[7] or Luquasorb from BASF[8]). However, these matrices do not have a good biodegradability, so they have to be removed from the field once they have acted in order to avoid toxicity problems. A possible alternative to these SAP matrices is the use of biodegradable superabsorbent

(bio)polymeric (SAB) matrices, which have a high biodegradability and no toxicity[9].

Among all the materials that can be used to elaborate SAB matrices, proteins have technological, economic and environmental advantages. On the one hand, there is a considerable potential to modulate their properties due to their great variability in amino acid composition, the wide range of potential formulations and the wide variety of applicable processing techniques[10]. In addition, they are the most underutilized and undervalued by-product in the agri-food industry, thus their use as SAB materials implies an increase in their added value[11]. Finally, they can pose an extra contribution of nutrients after their degradation due to their significant nitrogen content. All this makes protein-based SAB matrices have a great potential for their use in horticulture; however, this use is still limited by the lack of knowledge in the formulation and processing thereof.

Another advantage that these protein-based SAB matrices could provide for their use in horticulture is the incorporation of micronutrients to crops in a controlled manner. In this sense, the micronutrients would be incorporated into the protein-based SAB matrices thought soluble salts already used in horticulture which could be released from the matrices due to their biodegradation and the release of water, thus being able to be captured by the plant. In this way, there would be an increase in the efficiency of incorporating micronutrients due to they would be incorporated in a controlled manner, avoiding the typical excesses of conventional fertilization, which causes the

contamination of soil and groundwater by excess nutrients[12,13]. One of the micronutrients that generate the most pollution problems is zinc. This is due to the great solubility of the salts used for the incorporation of this micronutrient[14]. In this sense, the incorporation of zinc into the protein-based SAB matrices, and its extrapolation to the other essential micronutrients, would pose an added value, increasing its interest while replacing the commercial SAP matrices.

From all the different proteins studied in the literature for the elaboration of protein-based SAB matrices (based on pea[15], egg albumen[16], crayfish[17], rice[18], soy[19], whey[20]), soy protein has proven to be the one with the best absorbent capacity, due to its high content of glutamic and aspartic acid, which gives it a good hydrophilic character[21]. Furthermore, its high lysine content allows the introduction of some carboxylic groups, improving, even more, its hydrophilic character [22].

Among the fabrication methods, soy protein-based SAB matrices allow an adequate processing by injection molding, one of the most used techniques for the manufacture of synthetic plastics, which would facilitate its implementation on an industrial scale[21,23,24]. However, the incorporation of micronutrients generally hinders the processing of these matrices, as it results in a reduction in the strengthening potential of the matrix associated to the corresponding reduction in the protein content[25].

Therefore, the main objective of the present work is the development of suitable soy protein-based matrices with zinc chelated with 2,2',2'',2'''-(Ethene-1,2-

diyldinitrilo)tetraacetic acid (Zn EDTA), which is a salt that contains the essential micronutrient for plants. To achieve this objective, the mechanical and morphological properties of matrices with different concentrations of Zn EDTA incorporated throughout the processing stages (blends, bioplastic matrices and final matrices) as well as their water absorption capacity have been evaluated.

2. Materials and methods

2.1 Materials

Soy protein isolate (SPI) with min. 910 $g \cdot kg^{-1}$ protein, 60 $g \cdot kg^{-1}$ moisture and 30 $g \cdot kg^{-1}$ ash, which was supplied by Protein Technologies International (SUPRO 500E, Belgium) has been used to obtain protein-based SAB matrices. In addition, glycerol (Gly), provided by Panreac Química Ltd. (Spain) has been used as plasticizer. Finally, zinc chelated with 2,2',2'',2'''-(Ethene-1,2-diyldinitrilo)tetraacetic acid (Zn EDTA) has been used as a salt that provides the selected micronutrient, which was supplied by Trade Corporation International S.A.U. (Spain).

2.2 Preparation of soy protein-based matrices

A generic two-stage procedure (Figure 1) was followed to obtain soy protein-based matrices with Zn EDTA incorporated. The process consisted in an initial homogenization which was carried out with a two-blade counter-rotating mixer Polylab QC (ThermoHaake, Germany). The mixing was performed adiabatically for 10 min, at 50 rpm and at room temperature (25 ± 2 ºC) following the same protocol used in SPI/Gly blends previously studied[24,26]. A constant ratio (1:1)

between SPI and Gly and different concentrations of Zn EDTA (50, 100 and 150 $g \cdot kg^{-1}$) were used. The SPI/Gly blend without Zn EDTA was selected as reference (Ref.). During this mixing, both torque variation (M) and temperature evolution ($\Delta T = 100 \cdot (T-T_0)/T_0$, where T is the temperature at time of measurement and T_0 is the initial temperature) were studied.

Consecutively, an injection molding of the blends was carried out in order to obtain rectangular bioplastic matrices (60x10x1 cm). Thus, the blends were introduced in a MiniJet Piston Molding System II (ThermoHaake, Germany) where they were injected through a nozzle into a previously heated mold. The parameters in this stage were selected based on the rheological characterization of the blends and previous studies carried out to optimize the water uptake capacity of SPI/Gly systems[21]: a cylinder and mold temperature of 40 and 70 ºC, respectively, an injection pressure of 500 bar (for 20 s) and a post-injection pressure of 200 bar (for 300 s).

Finally, a dehydrothermal treatment (DHT) was carried out before performing the water uptake capacity tests according to the ASTM 180 D570 standard[27]. In addition, it was found that without this stage the bioplastics' network is not strong enough and they disintegrated in the water. This treatment consisted of introducing the bioplastic matrices in a conventional oven at 50.0 ± 0.1 ºC for 24 h.

2.3 Characterization of the soy protein-based systems with Zn EDTA

A complete characterization of the systems was carried out in order to evaluate the suitability of the matrices as superabsorbent materials with incorporated micronutrients. Thus, the blends were evaluated to optimize their processing, as well as the bioplastic matrices before and after a severe treatment with water to study their properties. It is worth mentioning that the matrices after the severe treatment with water were dried by a freeze-drying process to obtain dry matrices that can be characterized.

2.3.1 *Thermomechanical tests of the blends.*

The homogenized blends were mechanically characterized by small amplitude oscillatory compression tests, using a mechanical dynamic analyzer RSA3 (TA Instruments, USA) with a plate-plate geometry of 8 mm in diameter. The purpose of these tests was to define the behavior of the blends with the temperature to select the optimal treatment in the subsequent injection molding. Thus, temperature ramp tests between 25 and 120 ºC were performed, at 1 Hz and a strain within the linear viscoelastic range (0.01%), where the elastic modulus (E') and the loss tangent (tan δ = E''/E') were studied throughout the temperature range selected.

2.3.2 *Thermogravimetric analysis (TGA)*

The thermogravimetric analyses (TGA) were carried out using a thermogravimetric analyzer Q600 (TA Instrument Inc., USA) in order to study the thermomechanical stability of the different raw materials, a homogeneous blend of them and a matrix after water absorption. In these analyses, the

samples were introduced into the equipment at a temperature of 25 ºC, and then they were raised to a temperature of 600 ºC at a speed of 10 ºC/min. During the test, the samples were kept in a nitrogen atmosphere, and their weight variation was measured.

2.3.3 *Tensile strength measurements*

The tensile tests were performed on a mechanical dynamic analyzer RSA3 (TA Instruments, USA) following a modified protocol of the ISO standard 527-2:1993[28] with the purpose of evaluating the mechanical resistance of the different bioplastic matrices. Therefore, the bioplastic matrices were subjected to an increasing axial stress until breakage at a crosshead speed of 1 mm/min, studying the relationship between stress (σ) and strain (ε). In addition, the strain at break (ε_{max}), maximum stress (σ_{max}) and Young's modulus of the different bioplastic matrices were evaluated.

2.3.4 *Water uptake capacity and soluble matter loss*

Water uptake capacity and soluble matter loss from the different bioplastic matrices were measured to determine whether the matrices with Zn EDTA incorporated have a superabsorbent character. To perform this measurements, a modification of the ASTM 180 D570 standard[27] was followed, introducing the bioplastic matrices in a closed vessel with 300 mL of distilled water for 24 h.

Then, the water uptake capacity was obtained following equation 1:

$$Water\ uptake\ capacity\ (g \cdot kg^{-1}) = \frac{w_2 - w_3\ (g)}{w_3\ (kg)} \qquad (1)$$

Where w_2 is the weight of the matrix after the absorption stage and w_3 is the weight of the matrix after the freeze-drying stage (-80 ºC and <15 Pa in a LyoQuest freeze-drying equipment (Telstar, Spain). This freeze-dried was chosen as the drying step because it allows maintaining the structure of the matrices after water absorption for a subsequent characterization thereof.

Finally, soluble matter loss was calculated following equation 2:

$$Soluble\ matter\ loss\ (g \cdot kg^{-1}) = \frac{w_1 - w_3\ (g)}{w_1\ (kg)} \qquad (2)$$

Where w_1 is the weight of the bioplastic matrices after the dehydrothermal stage.

2.3.5 *Scanning electron microscopy (SEM)*

SEM micrographs were made in order to compare the structures of the different bioplastic matrices before and after the water absorption and freeze-drying step, following the same protocol studied by Orawan et al.[29]. First, a palladium/gold sputtering was performed to improve the electrical conduction of the bioplastic matrices and enhance the quality of the micrographs. Finally, the bioplastic matrices were observed through a Zeiss EVO electronic microscope (USA) with an acceleration voltage of 10 kV.

2.3.6 *Inductively coupled plasma-atomic emission spectroscopy (ICP-AES)*

Measurements of inductively coupled plasma-atomic emission spectroscopy (ICP-AES) were made to the matrices with different zinc concentrations in an ICP SpectroBlue TI (Spectro, Germany). In this sense, it was possible to

evaluate the amount of zinc that was released from the matrix in the exiting water after absorption and the amount of zinc that remained in it.

To carry out these measurements, the matrices were first subjected to a pretreatment, in which they were digested with acids (HNO_3 and H_2O_2 in a 7:1 ratio) obtaining a solution. Subsequently, the different solutions passed through a nebulizer to form a spray that was dragged with an argon stream towards a plasma torch. This torch that was at a temperature of around 6000 K, dissociating the spray into free atoms and ions that emit in characteristic wavelengths, which were measured to determine the concentration of each element.

2.3.7 *Mechanical measurements*

Mechanical measurements were made to determine the mechanical resistance of the matrices after the soluble matter loss, which was carried out in the water absorption, since when loss occurs there is more free volume in the matrices, thus their mechanical properties are expected to decrease.

These measurements were made in compression mode using a mechanical dynamic analyzer RSA3 (TA Instruments) with a plate-plate geometry of 8 mm in diameter. Frequency sweep tests were performed between 0.02 and 20 Hz, at a strain within the linear viscoelastic range (0.01%) and room temperature (25 ± 2 ºC) to study the variation of the elastic (E') and viscous (E'') moduli with the frequency.

2.4 Statistical analysis

At least three replicates of each measure were made. Statistical analyzes were carried out with t test and one-way analysis of variance (p <0.05). For this, PASW Statistics for Windows (Version 18: SPSS, Chicago, IL) was used. In addition, the standard deviation of the selected parameters was calculated.

3. Results and discussion

3.1 Preparation of soy protein-based matrices

Figure 2 shows the parameters evaluated during the mixing of the blends with different percentages of Zn EDTA (50, 100 and 150 $g \cdot kg^{-1}$), using as reference the blend without Zn EDTA. Figure 2A shows the evolution of the torque (M) with the mixing time (t) of the different blends. All the systems followed the same evolution in M, where a maximum peak was first observed, attenuated to a value that remained constant during the mixing time. The incorporation of 50 $g \cdot kg^{-1}$ Zn EDTA registered the lowest torque values compared to the systems produced with 100 or 150 $g \cdot kg^{-1}$ Zn EDTA content. However, the values obtained for these systems were lower than the torque values for the reference system (Ref.). This behavior may be due to the lower SPI and Gly concentration of the systems when Zn EDTA is incorporated. Zn EDTA can be attenuated by Gly in small percentages; however, by increasing its percentages, part of this acts as a filler material, making the blend more compact and therefore increasing its mixing torque again.

On the other hand, Figure 2B shows the temperature evolution ($\Delta T = 100 \cdot (T-T_0)/T_0$) recorded during the mixing time (t). All the systems showed a growth of

ΔT with the mixing time, produced by the proper mixing since it was mixed adiabatically. As can be observed, the incorporation of Zn EDTA led to a slighter increase in ΔT, although once again, lower than the ΔT registered by the reference system. It is worth pointing out the system with 150 $g \cdot kg^{-1}$ Zn EDTA, which overcame the ΔT registered by the reference system after 6 minutes of mixing, probably due to the greater amount of material that acts as filler, as already mentioned with the torque.

The blends, once mixed, were mechanically characterized. Figure 3 shows the evolution of the elastic modulus (E') and the loss tangent (tan δ) with the temperature applied in the compression tests. The most remarkable difference is the increase in the values of E' with the incorporation of Zn EDTA into the system, possibly due to a restructuring produced between the protein and the salt. However, all the systems exhibited a similar behavior at the beginning, where a progressive decrease of E' took place until reaching an inflection point, more or less pronounced depending on the blend, at a temperature close to 70 ºC. This point, at which a maximum in tan δ was obtained, corresponds to the glass transition temperature of the blends, where the material is more processable and, consequently, a more effective injection molding of the blends could be achieved. After this point, two different behaviors can be assessed depending on the presence or absence of Zn EDTA on the blend. On the one hand, the blend without Zn EDTA continued with a progressive decrease in E', whereas, on the other hand, blends containing Zn EDTA showed a rise of E' up

to a maximum. This rise of E' may be due to a strengthening of the matrix with the addition of Zn EDTA. This incorporation can form a metalloprotein, making the structure better. However, it did not affect the maximum found for tan δ, which made it possible to inject all the blends at the same temperature (70ºC), as previously described in the Experimental section.

3.2 Characterization of soy protein-based bioplastic matrices with Zn EDTA

3.2.1 *Thermogravimetric analysis (TGA)*

Figure 4 shows the thermogravimetric analyses of the different raw materials (SPI, Gly, Zn EDTA), a homogenized blend of them and a matrix after water absorption. As can be observed in the TGA profiles, the protein isolate (SPI) has a first weight loss between 50 and 100 ºC, which is due to the evaporation of the water it contained. In addition, it has a more pronounced loss between 200 and 450 ºC, which corresponds to the denaturation of the protein. As for Gly, it only presents a single weight loss between 200 and 280 ºC, which corresponds to the evaporation of glycerol. This profile suggests that, although glycerol is a very hygroscopic material, it does not present humidity. Similar data have been obtained in the literature [24]. On the other hand, the Zn EDTA profile has several weight losses. The first losses were recorded between 50 and 200 ºC, which may correspond to a breakdown in the complex formed between Zn and EDTA. Then, a more pronounced weight loss is observed at a temperature between 350-450 ºC due to the decomposition of part of the EDTA, which is reported in the literature [30]. It should be noted that, among all the raw

materials used, only glycerol was totally lost at 600 ºC, leaving 28.7% of SPI and 54.9% of Zn EDTA.

Regarding the homogeneous blends of the different components (450, 450 and 100 $g \cdot kg^{-1}$ of SPI, Gly and Zn EDTA, respectively), different weight losses can be observed, corresponding to each of the raw materials. Thus, the SPI peak is between 200 and 450 ºC and the Gly peak between 200 and 280 ºC. As for the Zn EDTA, a first peak between 50 and 100 ºC is observed, which overlaps with the possible humidity of the sample, and another slightly pronounced peak between 350 and 400 ºC. The first peak observed at 50-100 ºC is the possible cause of the strengthening observed previously in thermomechanical tests. The release of water from the protein linked to the possible breakdown of the Zn EDTA complex would cause the structure to form new bonds (metalloprotein) reinforcing and obtaining an improvement of the elastic modulus (E').

Finally, in the profile of the matrix after the water treatment, the weight loss that corresponds to Gly does not appear, thus it is assumed that all Gly was released to the water due to its great hygroscopic character. Regarding the peaks corresponding to the SPI and Zn EDTA, these still appear, thus these materials are present after water absorption.

3.2.2 *Tensile strength measurements*

The results from tensile strength measurements of the bioplastic matrices with different percentages of incorporated Zn EDTA (50, 100 and 150 $g \cdot kg^{-1}$), as well as those without Zn EDTA for the reference (Ref.) can be observed in Figure 5.

Figure 5A shows the relationship between stress (σ) and strain (ε) in the different bioplastic matrices. All the bioplastic matrices had a first elastic zone, where the strain could be recovered over time. In this zone, a lineal relationship was maintained between strain and stress, thus making it possible to obtain the Young's modulus of the different matrices. Then, a plastic area was recorded, which remained until the breakage of the bioplastic matrices. Once the elastic zone was overcome, the matrices did not recover their shape. The incorporation of 50 $g \cdot kg^{-1}$ Zn EDTA improved the maximum strain, without modifying the maximum stress reached. However, this improvement was not observed when higher percentages of Zn EDTA were incorporated. As previously mentioned, this fact is possibly due to the action of Zn EDTA as a filler in these bioplastic matrices, which did not cross over with the protein structure. In addition, it can hinder the crosslinking of the protein, which is also in smaller proportion, therefore the bioplastic matrices have worse mechanical properties in these cases.

On the other hand, Figure 5B shows the parameters of strain at break (ε_{max}), maximum stress (σ_{max}) and Young's modulus of the different bioplastic matrices studied without Zn EDTA (Ref.) and with different Zn EDTA concentrations (50, 100 and 150 $g \cdot kg^{-1}$) to compare their mechanical properties. As can be observed σ_{max} did not show significant differences between the reference bioplastic matrix (Ref.) and bioplastics with 50 $g \cdot kg^{-1}$Zn EDTA. However, matrices with higher Zn EDTA concentrations (100 and 150 $g \cdot kg^{-1}$) showed

lower σ_{max} values, which were more pronounced for the system with the highest Zn EDTA concentration. As for ε_{max}, an increase was observed with the incorporation of 50 $g \cdot kg^{-1}$ Zn EDTA, which decreased significantly when incorporating larger amounts of Zn EDTA. Finally, the Young's modulus did not present significant differences in the studied systems except, once again, for the bioplastic matrix that contains 50 $g \cdot kg^{-1}$ Zn EDTA that improved slightly. This behavior is consistent with the theory that in concentrations above 50 $g \cdot kg^{-1}$Zn EDTA, there is a greater amount of filler material incorporated, leading to worse mechanical properties due to this extra material do not allow to form the protein network of the matrices.

3.2.3 *Water uptake capacity and soluble matter loss*

Figure 6 shows both the water uptake capacity and the soluble matter loss. The matrix without salt showed values slightly lower than the limit of the superabsorbent materials (10000 $g \cdot kg^{-1}$). However, the incorporation of Zn EDTA increased the water absorption capacity of the bioplastic matrices, which was more pronounced at higher percentages, being able to consider these materials as superabsorbents. Although, the bioplastic matrix with 150 $g \cdot kg^{-1}$ Zn EDTA, which had the best water uptake capacity, was not resistant out of the water, even breaking down, possibly due to its lower amount of protein, which may have caused the matrix to be less structured. Regarding soluble matter loss, there were no significant differences between the different systems, which concludes that Gly is lost in all systems due to its high hydrophilic character, as

previously confirmed with TGA (3.2.1). In addition, the protein/Zn EDTA loss increased when larger amounts of Zn EDTA were incorporated since these matrices had less Gly, although these systems reached practically the same soluble matter loss. This may be due to the lower strengthening of the matrices, as mentioned above. However, the protein/Zn EDTA ratio that was lost could not be estimated until ICP-AES analyzes were carried out.

3.3 Characterization of soy protein-based matrices with Zn EDTA

Once the bioplastic matrices were subjected to a water absorption step, followed by a freeze-drying stage, the morphological and mechanical properties of the final matrices were studied to analyze the possible variation that this stage confers to the matrices.

3.3.1 *Inductively coupled plasma-atomic emission spectroscopy (ICP-AES)*

Table 1 shows both the amount of zinc in the bioplastic matrices before and after the absorption stage, with the latter being measured by ICP-AES. The amount of zinc remaining in the matrices after the absorption stage did not present significant differences between the matrices. Therefore, the zinc released in the water absorption stage was more pronounced as more Zn EDTA was incorporated into the initial bioplastic matrix. This fact may be due to the lower structuring of the matrix, as has already been mentioned, which caused the loss of a greater amount of protein and Zn EDTA, as already observed in the soluble matter loss measurements.

With respect to these results, it is expected that in all the matrices, most of the zinc would be released in a controlled manner with the water incorporated in the matrix, with this percentage being more pronounced in the matrix with higher Zn EDTA incorporated. Moreover, the small amount of Zn retained in the matrix would be released along with the other nutrients provided by the protein matrix (mainly nitrogen) during its biodegradation.

3.3.2 *Scanning electron microscopy (SEM)*

Figure 7 shows the micrographs taken from the different samples. The images of the bioplastic matrices (Figures 7A, 7C, 7E, 7G) show that the addition of Zn EDTA to the bioplastic matrices made their structure more homogeneous, with less pores in it. This could be due to the greater amount of solid material in the systems, with part of it acting as a filler material. On the other hand, the images captured from the matrices (Figures 7B, 7D, 7G, 7H) show how the passage through the stages of water absorption and freeze-drying made the matrices develop larger and more heterogeneous pores, which is more evident at the higher concentrations of Zn EDTA. This behavior could be due to the greater soluble matter loss there was as more salt (filler material) was incorporated into the matrix, which was anticipated in previous tests.

In this sense, the filler material made the structure develop fewer holes in the bioplastic matrices. However, most of this material was lost in the water absorption stage, due to the lower structuring of the protein matrix, making the matrices with greater concentrations of Zn EDTA, present more holes (free

volume) after absorption. Thus, the matrix obtained after incorporating 50 $g \cdot kg^{-1}$ of Zn EDTA is the one with the lowest free volume and the most heterogeneous pores. This could explain the improvement of the mechanical properties of the bioplastic matrices when 50 $g \cdot kg^{-1}$ of Zn EDTA was incorporated, since they have a defined, consolidated and reinforced structure. Furthermore, these matrices possibly have better mechanical properties after absorption.

3.3.3 *Mechanical measurements*

The mechanical properties of the matrices after absorption can be seen in Figure 8. This figure shows the evolution of the elastic (E') and viscous (E'') moduli in the frequency range studied for the matrices with different percentages of Zn EDTA (50, 100 and 150 $g \cdot kg^{-1}$) incorporated, using the matrix without Zn EDTA as reference (Ref.).

As can be observed, E' remained above E'' for all the frequency range studied. Moreover, E' had a slight dependence on frequency. Thus, all the matrices showed a basically elastic character. In fact, stronger matrices (higher E' values) were obtained when Zn EDTA was incorporated. In addition, E'' presented greater variations, possibly due to the low stability of the matrices after water absorption. Once again, matrices with Zn EDTA incorporated also had higher E'' values than the reference system.

4. Conclusions

Superabsorbent soy protein-based matrices have been developed, showing a great potential for their use in horticulture. In addition, essential micronutrients for crops (zinc) can be incorporated in them.

The addition of zinc chelated with 2,2',2'',2'''-(Ethene-1,2-diyldinitrilo)tetraacetic acid (Zn EDTA) to the matrices improved their superabsorbent capacity and their mechanical properties up to a concentration of 50 $g \cdot kg^{-1}$ Zn EDTA. In addition, the microstructure of bioplastic matrices with Zn EDTA incorporated is more homogeneous due to their greater amount of filler material. However, after introducing them into the water absorption stage, these matrices present a greater free volume due to a greater soluble matter loss.

Zinc is mostly released with water when the latter leaves the matrix in a controlled manner. However, a small amount is retained in the matrix, to be releasedit during its biodegradation. Thus, there is a first faster release of zinc, when water is incorporated into the crop and a slower second release of zinc along with the rest of the nutrients of the protein matrix conditioned by its biodegradability. This release profile can benefit the crops, since most of the zinc is needed in the growth stage, which occurs in the first days, and a lower quantity is required during maturation.

Further studies will be needed required in the future to analyze the release and plan assimilation of water and zinc in normal horticultural conditions.

5. Acknowledgments

This work is part of a project funded by MINECO/FEDER (Ref. CTQ2015-71164-P), the authors gratefully acknowledge their financial support. The authors also acknowledge for the pre-doctoral grant from Mercedes Jiménez-Rosado (FPU2017/01718-MEFP) and Víctor Perez-Puyana (VPPI-US). Finally, the authors thanks CITIUS for their access and assistance to the Microanalysis and Microscopy services.

6. References

1 Cox PM, Betts RA, Jones CD, Spall SA, and Totterdell IJ. Acceleration of global warming due to carbon-cycle feedbacks in a coupled climate model. *Nature* Macmillan Magazines Ltd.; **408**:184–187 (2000).

2 Wang X, Auler AS, Edwards RL, Cheng H, Ito E, and Solheid M. Interhemispheric anti-phasing of rainfall during the last glacial period. *Quat Sci Rev* **25**:3391–3403 (2006).

3 Venuprasad R, Lafitte H, and Atlin G. Response to direct selection for grain yield under drought stress in rice. *Crop Sci* **47**:285–293 (2007).

4 Johnson MS and Leah RT. Effects of superabsorbent polyacrylamides on efficiency of water use by crop seedlings. *J Sci Food Agric* **52**:431–434 (1990).

5 Chanda M and Roy K. Plastics Technology Handbook. 4th ed. Boca Raton: CRC Press; 2007.

6 Zohuriaan-Merh MJ and Kabiri K. Superabsorbent polymer materials: a review. *Iran Polym J* **17**:451–477 (2008).

7 Evonik. Creasorb: superabsorbents for non-sanitary applications. 2017. Available: https://www.creasorb.com/product/creasorb/en/about/ [16 November 2018].

8 Chempoint. BASF superabsorbent polymers. 2018. Available: https://www.chempoint.com/products/catalog/basf/basf-superabsorbent-polymers [16 November 2018].

9 Mortain L, Dez I, and Madec PJ. Development of new composites materials, carriers of active agents, from biodegradable polymers and wood. *Comptes Rendus Chim* **7**:635–640 (2004).

10 Bozell JJ. Feedstocks for the Future: Using Technology Development as a Guide to Product Identification. *Feedstocks for the Future* p. 1–12 2006.

11 Damodaran S. Food Proteins and Their Applications. New York: Routledge; 1997.

12 Muscanescu A. Organic versus conventional: advantages and disadvantages of organic farming. *Econ Eng Agric Rural Dev* **13**:253–256 (2013).

13 Timilsena YP, Adhikari R, Casey P, Muster T, Gill H, and Adhikari B. Enhanced efficiency fertilisers: A review of formulation and nutrient release patterns. *J Sci Food Agric* **95**:1131–1142 (2015).

14 Alloway BJ. Micronutrients and Crop Production: An Introduction. In: Alloway BJ, ed. *Micronutrient Deficiencies in Global Crop Production* Dordrecht: Springer Netherlands; p. 1–39 2008.

15 Perez-Puyana V, Felix M, Romero A, and Guerrero A. Development of pea protein-based bioplastics with antimicrobial properties. *J Sci Food Agric* **97**:2671–2674 (2017).

16 Jones A, Zeller M, and Sharma S. Thermal, mechanical, and moisture absorption properties of egg white protein bioplastics with natural rubber and glycerol. *Prog Biomater* **2**:12 (2013).

17 Felix M, Romero A, Cordobes F, and Guerrero A. Development of crayfish bio-based plastic materials processed by small-scale injection moulding. *J Sci Food Agric* **95**:679–687 (2014).

18 Félix M, Lucio-Villegas A, Romero A, and Guerrero A. Development of rice protein bio-based plastic materials processed by injection molding. *Ind Crop Prod* **79**:152–159 (2016).

19 Liu W, Misra M, Askeland P, Drzal LT, and Mohanty AK. 'Green' composites from soy based plastic and pineapple leaf fiber: fabrication and properties evaluation. *Polymer (Guildf)* **46**:2710–2721 (2005).

20 Montaño-Leyva B, Silva GGD da, Gastaldi E, Torres-Chávez P, Gontard N, and Angellier-Coussy H. Biocomposites from wheat proteins and fibers: Structure/mechanical properties relationships. *Ind Crops Prod* **43**:545–555 (2013).

21 Fernández-Espada L, Bengoechea C, Cordobés F, and Guerrero A. Thermomechanical properties and water uptake capacity of soy protein-based bioplastics processed by injection molding. *J Appl Polym Sci*

133:43524 (2016).

22 Cuadri AA, Romero A, Bengoechea C, and Guerrero A. Natural superabsorbent plastic materials based on a functionalized soy protein. *Polym Test* **58**:126–134 (2017).

23 Félix M, Martín-Alfonso JE, Romero A, and Guerrero A. Development of albumen/soy biobased plastic materials processed by injection molding. *J Food Eng* **125**:7–16 (2014).

24 Fernández-Espada L, Bengoechea C, Cordobés F, and Guerrero A. Protein/glycerol blends and injection-molded bioplastic matrices: Soybean versus egg albumen. *J Appl Polym Sci* **133**:42980 (2016).

25 Jiménez-Rosado M, Pérez-Puyana V, Cordobés F, Romero A, and Guerrero A. Development of soy protein-based matrices containing zinc as micronutrient for horticulture. *Ind Crops Prod* **121**:345–351 (2018).

26 Felix M, Perez-Puyana V, Romero A, and Guerrero A. Production and Characterization of Bioplastics Obtained by Injection Moulding of Various Protein Systems. *J Polym Environ* **25**:91–100 (2017).

27 ASTM D570-98: Standard Test Method for Water Absorption Of Plastics. West Conshohocken: ASTM interntional; 2005.

28 ISO 570-2:1993, Plastics. Determination of tensile properties. Part 2: Test conditions for moulding and extrusion plastics. France: ISO/TC 46; 1993.

29 Orawan J, Scoottawat B, and Wonnup V. Effect to phosphate compounds on gel-forming ability of surimi from bigeye snapper (Priacanthus

tayanus). *Food Hydrocoll* **20**:1153–1163 (2006).

30 Oudghiri F, García-Morales JL, and Rodríguez-Barroso MR. Evaluation of sediments decontamination by chelating agents using thermogravimetric analysis. *Int J Environ Res* **9**:657–662 (2015).

Figure Captions

Figure 1: Different stages in the preparation of SAB protein-based matrices. Raw materials: soy protein isolate (SPI), glyerol (Gly) and Zn EDTA. DHT: dehydrothermal treatment.

Figure 2: Evolution of (A) mixing torque and (B) percentage ratio of increase in temperatura over mixing time process for soy protein isolate/glycerol/Zn EDTA blends at different zinc EDTA content (Ref., 50, 100 and 150 $g \cdot kg^{-1}$).

Figure 3: Dynamic mechanical thermal analysis results: Elastic modulus (E') and loss tangent (tan (δ)) for soy protein isolate/glycerol/Zn EDTA blends at different Zn EDTA content (Ref., 50, 100 and 150 $g \cdot kg^{-1}$).

Figure 4: Thermalgravimetric analysis tests for raw materials (SPI, Gly and Zn EDTA), a homogeneous blend of them (450, 450 and 100 $g \cdot kg^{-1}$ of SPI, Gly and Zn EDTA respectively) and a matrix after water absorption test (A) and their corresponding derivative signals (B).

Figure 5: Tensile strength measurements for soy protein isolate/glycerol/Zn EDTA bioplastics at different Zn EDTA contents (Ref., 50, 100 and 150 $g \cdot kg^{-1}$): (A) Stress-strain curves and (B) Parameters: maximum stress (σ_{max}), strain in the roture (ε_{max}) and Young's Modulus. Columns with different letters are significantly different ($p \leq 0.05$).

Figure 6: Water uptake capacity and soluble matter loss for soy protein isolate/glycerol/Zn EDTA matrices at different Zn EDTA contents (Ref., 50, 100 and 150 $g \cdot kg^{-1}$). Columns with different letters are significantly different ($p \leq 0.05$).

Figure 7: Scanning Electron Microscopy (SEM) micrographs of bioplastic matrices and matrices with different concentration of Zn EDTA (50, 100 and 150 $g \cdot kg^{-1}$). The matrix without salt is used as reference (Ref.).

Figure 8: Dynamic frequency sweep tests for soy protein isolate/glycerol/Zn EDTA matrices with diffetent Zn EDTA percentages (Ref., 50, 100 and 150 $g \cdot kg^{-1}$).

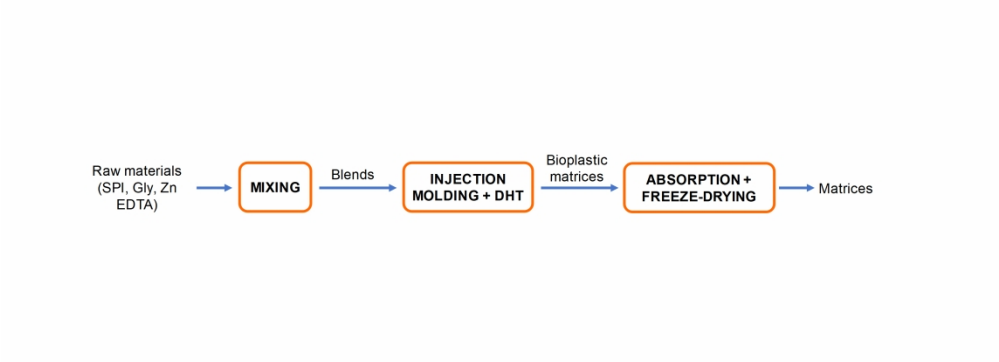

Figure 1: Different stages in the preparation of SAB protein-based matrices. Raw materials: soy protein isolate (SPI), glyerol (Gly) and Zn EDTA. DHT: dehydrothermal treatment.

296x108mm (300 x 300 DPI)

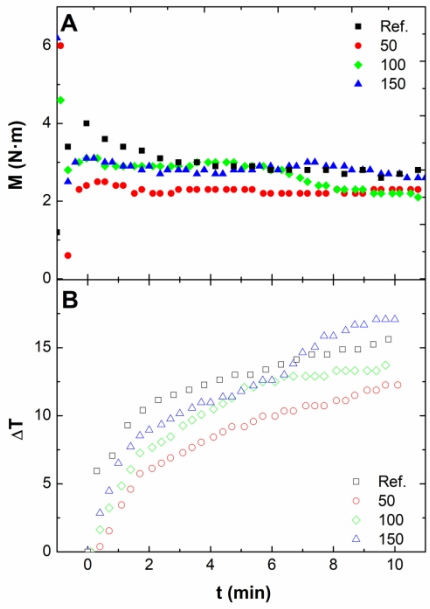

Figure 2: Evolution of (A) mixing torque and (B) percentage ratio of increase in temperatura over mixing time process for soy protein isolate/glycerol/Zn EDTA blends at different zinc EDTA content (Ref., 50, 100 and 150 g·kg-1).

290x203mm (300 x 300 DPI)

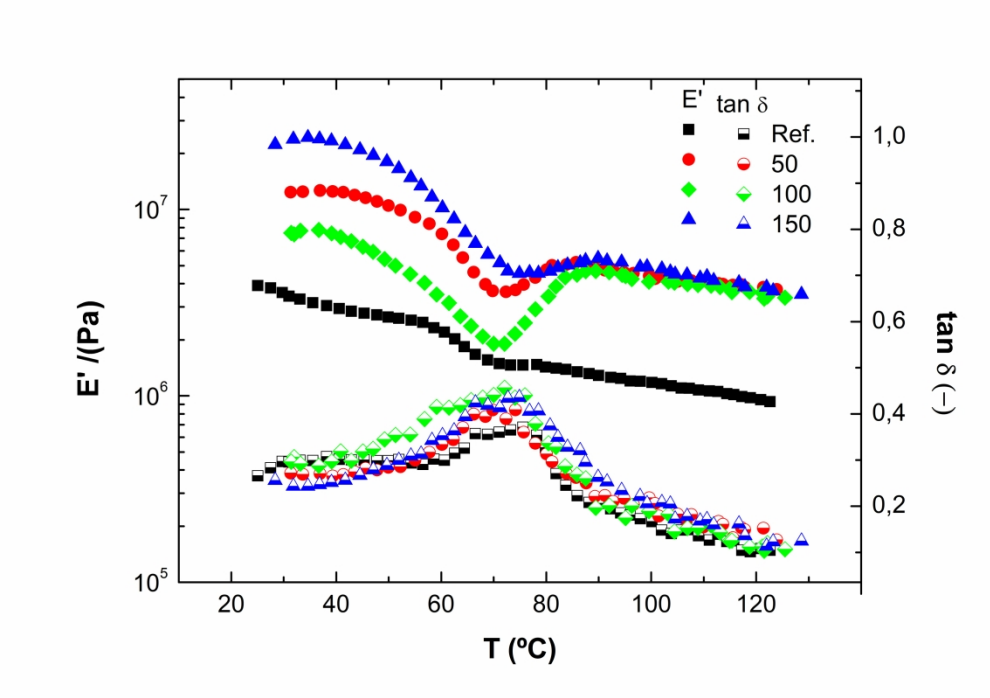

Figure 3: Dynamic mechanical thermal analysis results: Elastic modulus (E') and loss tangent (tan (δ)) for soy protein isolate/glycerol/Zn EDTA blends at different Zn EDTA content (Ref., 50, 100 and 150 g·kg-1).

290x203mm (300 x 300 DPI)

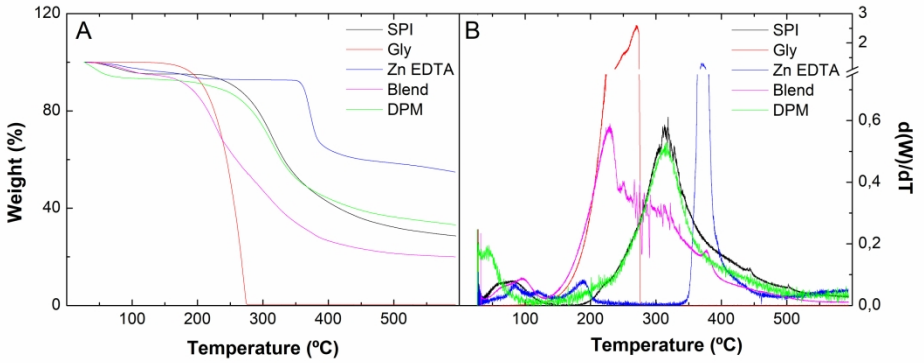

Figure 4: Thermalgravimetric analysis tests for raw materials (SPI, Gly and Zn EDTA), a homogeneous blend of them (450, 450 and 100 g·kg-1 of SPI, Gly and Zn EDTA respectively) and a matrix after water absorption test (A) and their corresponding derivative signals (B).

296x209mm (300 x 300 DPI)

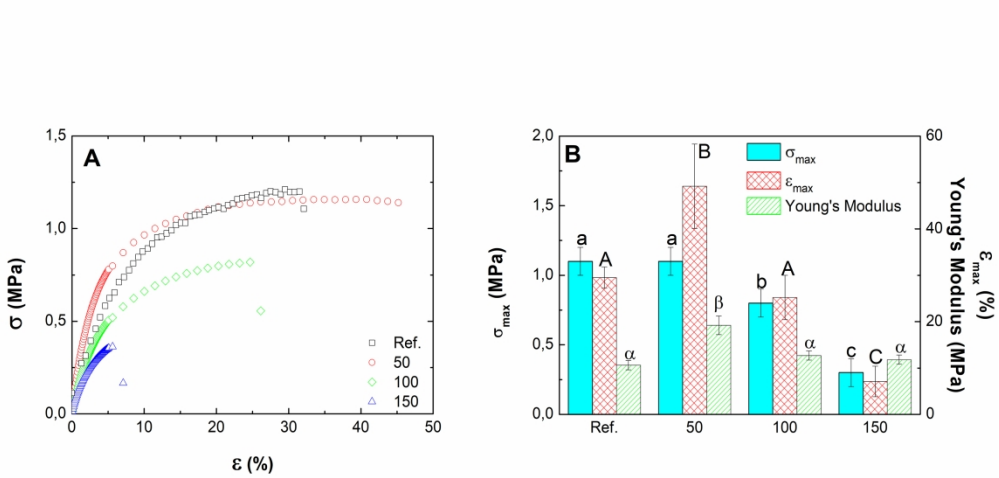

Figure 5: Tensile strength measurements for soy protein isolate/glycerol/Zn EDTA bioplastics at different Zn EDTA contents (Ref., 50, 100 and 150 g·kg-1): (A) Stress-strain curves and (B) Parameters: maximum stress (σmax), strain in the roture (εmax) and Young's Modulus. Columns with different letters are significantly different ($p \leq 0.05$).

290x203mm (300 x 300 DPI)

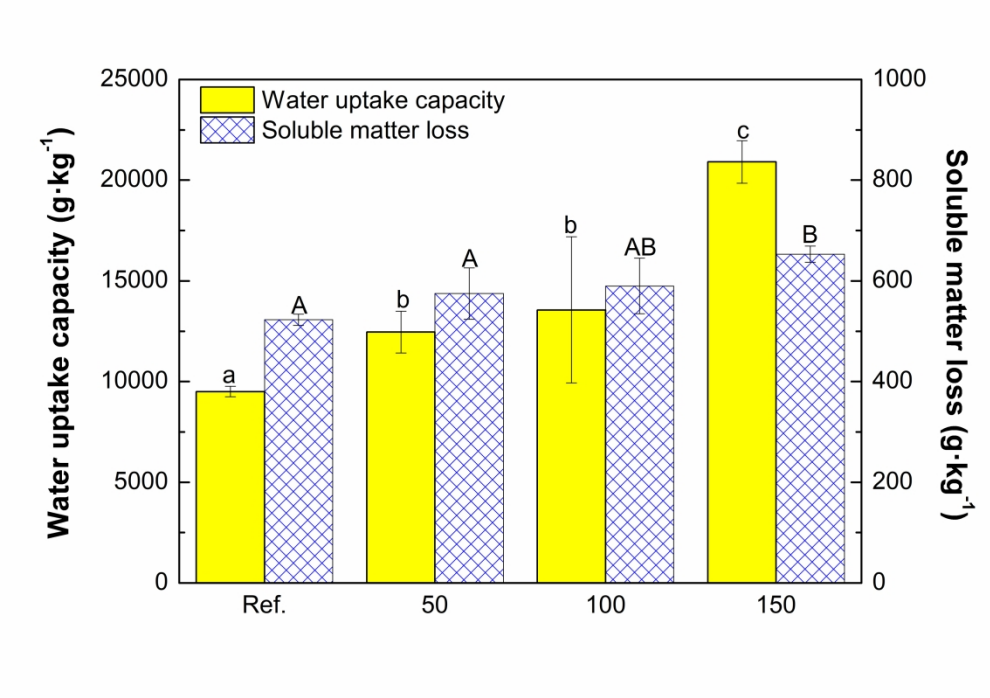

Figure 6: Water uptake capacity and soluble matter loss for soy protein isolate/glycerol/Zn EDTA matrices at different Zn EDTA contents (Ref., 50, 100 and 150 g·kg-1). Columns with different letters are significantly different ($p \leq 0.05$).

290x203mm (300 x 300 DPI)

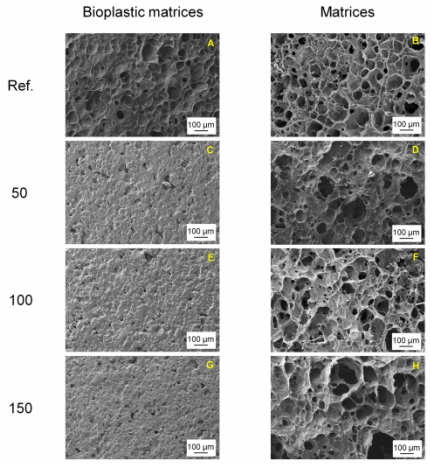

Figure 7: Scanning Electron Microscopy (SEM) micrographs of bioplastic matrices and matrices with different concentration of Zn EDTA (50, 100 and 150 g·kg-1). The matrix without salt is used as reference (Ref.).

296x209mm (300 x 300 DPI)

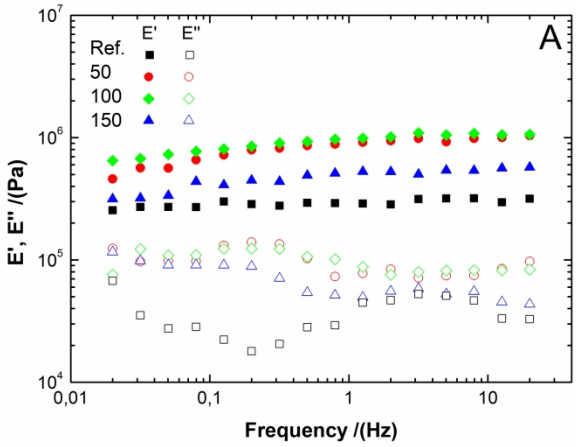

Figure 8: Dynamic frequency sweep tests for soy protein isolate/glycerol/Zn EDTA matrices with diffetent Zn EDTA percentages (Ref., 50, 100 and 150 g·kg-1).

296x209mm (300 x 300 DPI)

Tables

Table 1: Amount ($g \cdot kg^{-1}$) of zinc (Zn^{2+}) in the final matrix determined by ICP-AES measurements. Columns with different letters are significantly different ($p \leq 0.05$).

$g \cdot kg^{-1}$ Zn EDTA incorporated in the blends	**$g \cdot kg^{-1}$ Zn^{2+} in bioplastic matrices**	**$g \cdot kg^{-1}$ Zn^{2+} in matrices**
Ref.	-	-
50	9.14^{a}	0.87 ± 0.30^{b}
100	18.28^{c}	0.88 ± 0.66^{b}
150	27.42^{d}	0.88 ± 0.24^{b}